

# A Self-Diagnostic Adhesive for Monitoring Bonded Joints in Aerospace Structures

Yitao Zhuang<sup>\*a</sup>, Yu-hung Li<sup>a</sup>, Fotis Kopsaftopoulos<sup>a</sup>, Fu-Kuo Chang<sup>a</sup>

<sup>a</sup> Department of Aeronautics and Astronautics  
Stanford University, 496 Lomita Mall, Stanford CA 94305

## ABSTRACT

Bondline integrity is still one of the most critical concerns in the design of aircraft structures up to date. Due to the lack of confidence on the integrity of the bondline both during fabrication and service, the industry standards and regulations still require assembling the composite using conventional fasteners. Furthermore, current state-of-the-art non-destructive evaluation (NDE) and structural health monitoring (SHM) techniques are incapable of offering mature solutions on the issue of bondline integrity monitoring. Therefore, the objective of this work is the development of an intelligent adhesive film with integrated micro-sensors for monitoring the integrity of the bondline interface.

The proposed method makes use of an electromechanical-impedance (EMI) based method, which is a rapidly evolving approach within the SHM family. Furthermore, an innovative screen-printing technique to fabricate piezoelectric ceramic sensors with minimal thickness has been developed at Stanford. The approach presented in this study is based on the use of (i) micro screen-printed piezoelectric sensors integrated into adhesive leaving a minimal footprint on the material, (ii) numerical and analytical modeling of the EMI spectrum of the adhesive bondline, (iii) novel diagnostic algorithms for monitoring the bondline integrity based on advanced signal processing techniques, and (iv) the experimental assessment via prototype adhesively bonded structures in static (varying loads) and dynamic (fatigue) environments.

The proposed method will provide a huge confidence on the use of bonded joints for aerospace structures and lead to a paradigm change in their design by enabling enormous weight savings while maximizing the economic and performance efficiency.

**Keywords:** Bondlines, Structural health monitoring, Impedance, Damage index, piezoelectric, screen-printing

## 1. INTRODUCTION

Bondline integrity monitoring is still one of the most critical concerns in the design of aircraft and spacecraft structures up to date. Although adhesively bonded joints have demonstrated superior properties over mechanically fastened joints, current standards still require fasteners even with adhesive because of a lack of confidence on the integrity of the bondline in fabrication and during service. This reduces the benefits of bonding. There are two major types of defects in bondlines, gross defects and adhesive defects [1]. Debonds between adhesive/adherend and delamination on substrates, which fit into first category, can be detected via NDE methods like C-scan or ultrasonic reflection [2-5]. Those methods have been proven to be effective to a certain extent. However, specimen preparation takes a long time in all of these methods. Recent work in structural health monitoring, by Ihn and Chang [6-8], has demonstrated the ability to identify debonds in real-time, using built-in piezoelectric discs to generate ultrasonic waves.

An adhesive defect is seen as traction-free contacted surfaces, which show reduced bond strength and are difficult or impossible to detect using conventional NDE [5]. Kissing bonds are one of the major adhesive defects and possess little residual tensile or shear strength. Many factors may lead to kissing bonds, including surface contaminants, adhesive chemistry, inappropriate curing stress, residual stress, moisture ingress, etc. As a result, kissing bonds can appear in a local fashion and the only way to detect them is to measure the local adhesive during fabrication and in service to track its degradation [5, 9-17]. Kissing bonds are the most critical and challenging defect to be detected in bonded joints and

\* zyt@stanfor.edu; phone: (650) 723-3524

significantly influence the confidence of bondline integrity after the joints are placed in service.

Embedding micro/nano sensors inside the adhesive layer has the potential to be an effective solution to this challenge. Upon initial inspection, this approach may not seem feasible because adding new materials inside adhesive will increase the risk of contamination and introduce new defects. However, industry has begun to use adhesive films with fiber scrim inside, to ease handling and improve quality control. Relevant standards have been developed for this practice like BMS 5-121 TY.1. This indicates that this approach is feasible if shrinking the sensors down to the size of typical fibers and making them out of the same materials as current scrim so that the adhesive will have the same mechanical performance as well as the capability to monitor its own integrity degradation level can meet the standards.

## 2. METHOD OF APPROACH

In this section we present the development of a process to prepare the adhesively bonded aluminum single lap shear coupons with commercially available PZT sensors (3.1 mm or 1/8 inch diameter) embedded in the bondlines. After their fabrication, the coupons were loaded under static loading to study the response of the embedded sensors. Single lap joints with PZT sensors embedded were prepared to investigate the relationship between the electromechanical impedance behavior of the sensors and the load history across the lap joints (see Figure 1 and Figure 2). The samples were prepared following the ASTM D1002 (Standard Test Method for Apparent Shear Strength of Single-Lap-Joint Adhesively Bonded Metal Specimens by Tension Loading (Metal-to-Metal)), with 25.4 mm by 25.4 mm (1 inch by 1 inch) of bondline area for one sensor embedded.

Hysol EA 9696 adhesive film provided by Henkel was used to bond two aluminum alloy laps (2024 T5). Hysol EA 9696 is a modified epoxy film designed for applications requiring high toughness including aeronautics. The adhesive films are sealed and stored in the -18 °C freezer in Structures and Composites Lab at Stanford. The surface preparation procedure is designed to follow the ASTM standard D2651, Standard Guide for Preparation of Metal Surfaces for Adhesive Bonding.

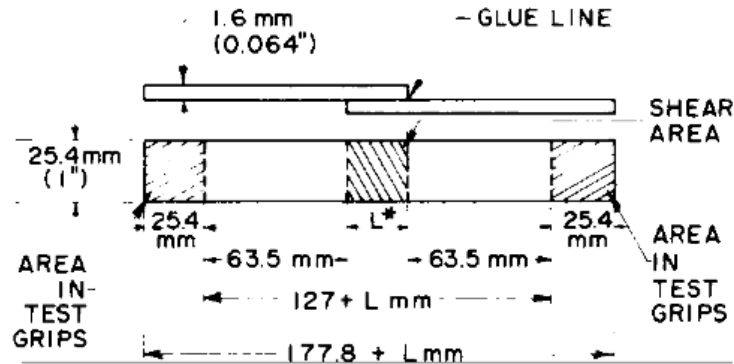


Figure 1. Suggested form and dimensions of test specimen of single lap joints from the ASTM D1002

Piezoelectric disc sensors fabricated by APC ceramics were embedded into the bondline. The piezo material was Navy II type equivalent PZT with 250 um in thickness and 3.1 mm (1/8 inch) in diameter. The material properties can be found in Table 1.

Table 1. The properties of the piezoelectric material in APC disc sensor

Density	Young's Modulus $E_{11}$	Young's Modulus $E_{33}$	Relative Dielectric Constant $K_T$	Piezo Charge Constant $d_{33}$	Piezo Voltage Constant $g_{33}$
7.6 g/cm <sup>3</sup>	63 GPa	54 GPa	1900	400 pC/N	24.8 mV-m/N

Due to the thickness of the piezoelectric disc sensors, three or four layers of adhesive film were used to fully encapsulate the sensors. Two varnished wires with diameter less than 100  $\mu\text{m}$  were also embedded to extend the two electrodes of the sensor to the outside of the bondline, which are subsequently connected to an impedance analyzer. The lay-up of the sample is illustrated in Figure 2. Following the instruction of the manufacturer, the samples were cured under vacuum for 90 minutes at 121  $^{\circ}\text{C}$ .

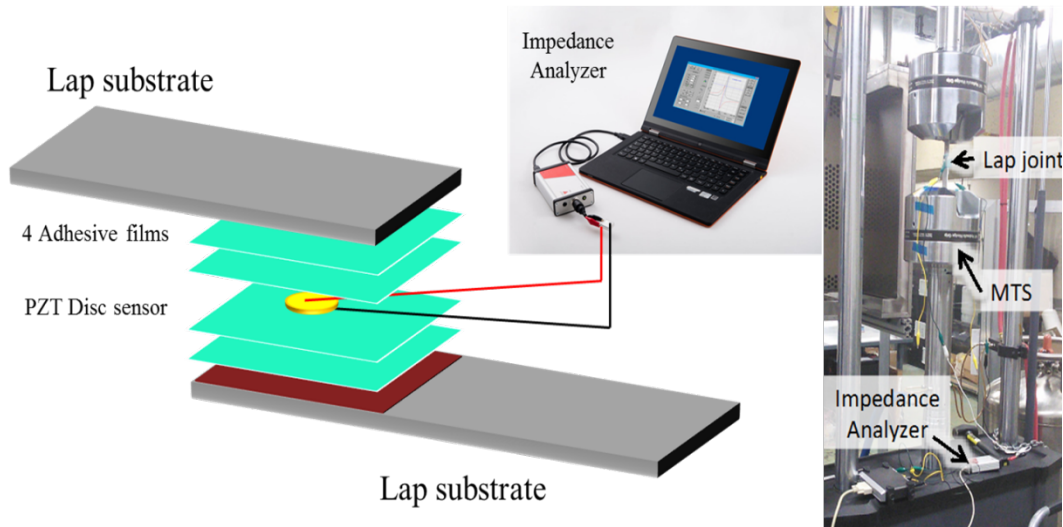


Figure 2. Illustration of a single lap joint with one piezoelectric sensor embedded in the adhesive bondline interface (left) and the experimental test setup (right).

### 3. RESULTS

#### 3.1 Impedance Behavior of Embedded Piezoelectric Sensors under Fatigue Loading

The sample was loaded on a MTS (Material Testing System) and a cyclic loading was introduced across the sample. The overall setup is shown in Figure 2. After a certain number of load cycles, the impedance was measured under the zero-loading condition by a SinePhase Z-check 16777k impedance analyzer. The impedance behavior of the piezo was recorded from 1 kHz to 3 MHz with an increment of 1 kHz. Both the real and imaginary impedance data were acquired as illustrated in Figure 3.

The sample was measured with a bondline thickness of 406  $\mu\text{m}$  (0.016 inch) with a variance of less than 25.4  $\mu\text{m}$  (0.001 inch). Graphite was used to contaminate the interface of adhesive and adherent. As a result, the bondline strength was measured at 500 psi [3.45 MPa] (29% of the nominal strength or 11.72 MPa [1700 psi]). The fatigue load was set to 3 Hz and the level of fatigue load was set to the range of 0 and 300 psi.

There were two resonance peak of impedance from 300 kHz to 2.5 MHz. The first one was around 900 kHz and the second one was around 1.8 MHz. The fatigue life was 48,000 cycles and before 36,000 cycles (75% of full fatigue life), the impedance of the embedded piezo-electric sensor almost overlapped as shown in blue color in Figure 3. After 36,000 cycles, the impedance started to deviate from its pristine state as shown in color of red. A close look around the first peak was illustrated in Figure 3, when the sample was approaching the end of fatigue life. The impedance deviated more from its pristine state with the increase of the number of the cyclic load.

The root mean square deviation (RMSD) was chosen as the damage index, which described the average impedance change from the baseline or the sample before any fatigue loading.

$$RMSD = \sqrt{\frac{\sum_{i=1}^N [Re(Z_h(\omega_i)) - Re(Z_u(\omega_i))]^2}{\sum_{i=1}^N [Re(Z_h(\omega_i))]^2}}$$

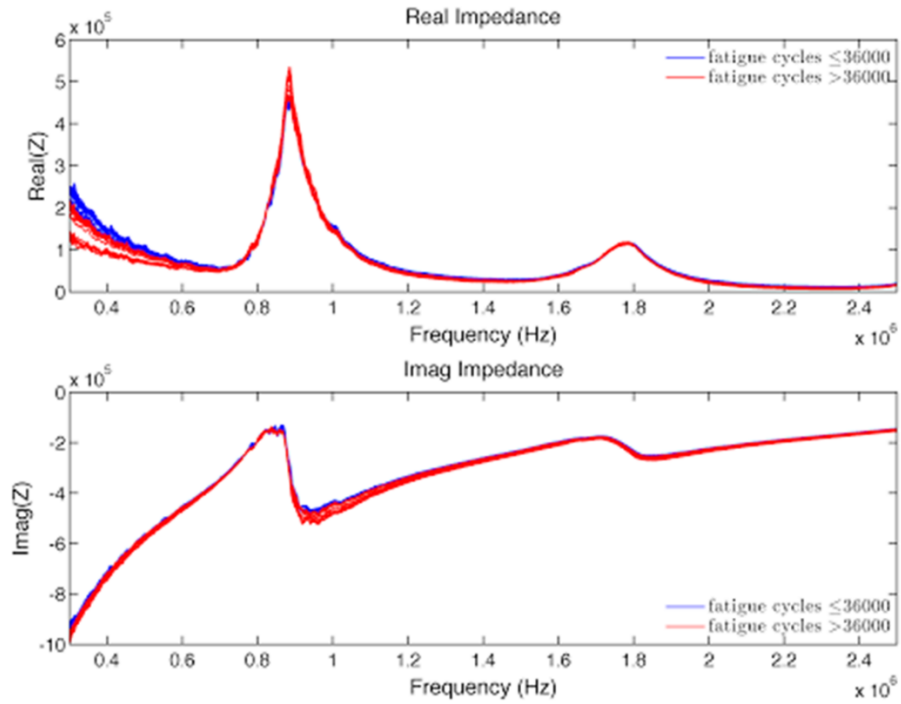


Figure 3: Real and imaginary parts of the electromechanical impedance of the embedded piezoelectric sensor in the adhesive bondline of the lap joint under fatigue loading.

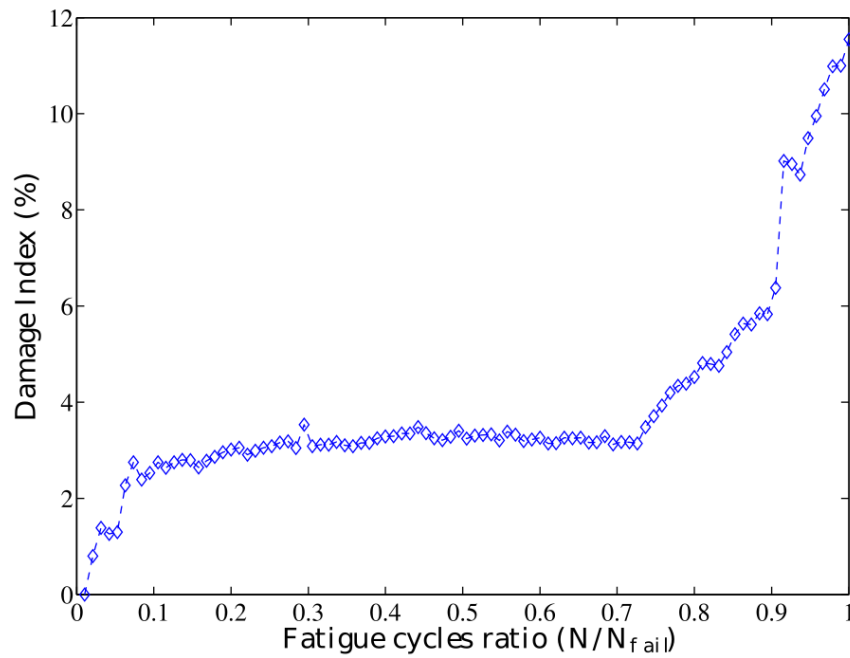


Figure 4: Damage index based on the root mean square deviation versus the number of fatigue cycles.

The RMSD between 800 kHz and 1 MHz was calculated and illustrated in Figure 4. Regardless of the impedance behavior after initial fatigue load, the impedance was relatively constant until around 42,000 cycles (88% of the fatigue life). After that, the damage index increased dramatically. The same trend was observed and reported by the author previously [18] for the embedded sensor in single lap joint under static loading and the impedance deviation was used to predict the strength of the bondlines. Similarly, the impedance of embedded piezo-electric sensor in bondlines and its evolution can be used as the indicator or pre-cursor of the failure of the adhesive under fatigue/dynamic loading.

### 3.2 Finite Element Simulation Study

The finite element model (FEM) has been developed in commercial software Abaqus 6.12 to simulate the impedance behavior of the embedded sensors in the bondlines, which provided a faster and more accurate result of the impedance of the large frequency bandwidth using the techniques of direct steady-state linear dynamic analysis. The element of C3D8E was used for the piezo-electric element and the mesh had a typical mesh dimension of 100  $\mu\text{m}$  to capture all the motion and deformation of the sensor.

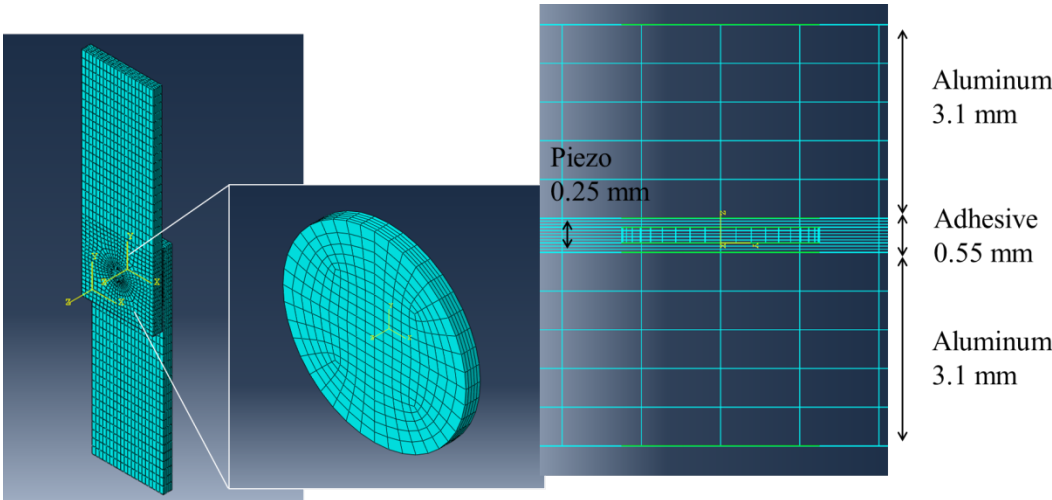


Figure 5: The FEM model and mesh of the bondline with embedded piezo sensor disc.

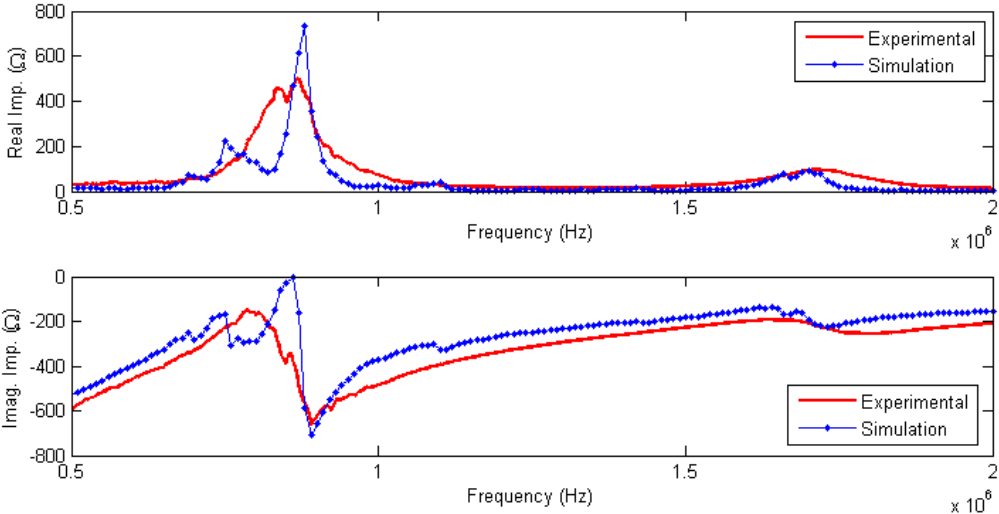


Figure 6. Comparison of numerically simulated and experimentally obtained impedance behaviour for a piezoelectric sensor embedded in the adhesive bondline.

The impedance from 50 kHz to 2 MHz was determined at the interval of 5 kHz. The results of both real and imaginary impedances are illustrated in Figure 6 in blue color. The experimental results are shown in red color. Without the further calibration of the material property as well as the dimension of the bondlines, the simulation matched the experimental result to certain extent in both frequency and amplitude.

Table 2: Material properties used in the numerical simulations.

Property	Unit	Aluminum Al 2024-T3	CFRP T800S/3900-2	Adhesive Hysol®EA 9696	Piezo PZT-5A
$E_{11}$	GPa	69.00	156.00	2.60	60.97
$E_{22}$	GPa	69.00	9.09	2.60	60.97
$E_{33}$	GPa	69.00	9.09	2.60	53.19
$G_{23}$	GPa	25.94	3.24	1.00	21.05
$G_{31}$	GPa	25.94	6.96	1.00	21.05
$G_{12}$	GPa	25.94	6.96	1.00	22.57
$\nu_{23}$		0.33	0.400	0.30	0.4402
$\nu_{13}$		0.33	0.228	0.30	0.4402
$\nu_{12}$		0.33	0.228	0.30	0.3500
$\rho$	kg m <sup>-3</sup>	2700	1540	1100	7750

$$d = \begin{bmatrix} 0 & 0 & 0 & 0 & 584 & 0 \\ 0 & 0 & 0 & 584 & 0 & 0 \\ -171 & -171 & 374 & 0 & 0 & 0 \end{bmatrix} \times 10^{-12} \text{ CN}^{-1} \quad \epsilon_{\sigma} = \begin{bmatrix} 1730 & 0 & 0 \\ 0 & 1730 & 0 \\ 0 & 0 & 1700 \end{bmatrix} \times \epsilon_0$$

In the literature, it was recommended that the kissing bond could be modeled by decreasing the stiffness of the interfacial element between adhesive and adherent [2,3]. The typical thickness of the element is 10 um. The stiffness of the interfacial element is tuned to different levels (10% to 90% of the original stiffness) to simulate the severity of the bondline degradation due to kissing bond as shown in Figure 7.

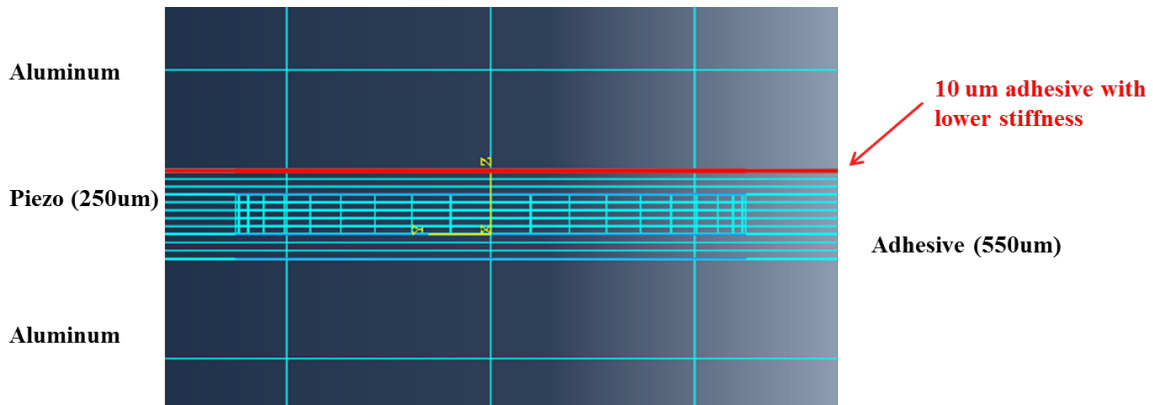


Figure 7. Kissing bond simulation is achieved via the reduction of the stiffness of the interfacial elements.

The dependence between damage index and the stiffness loss of the interfacial element is plotted in Figure 8. With increase of the stiffness loss, the corresponding DI increases dramatically. The trends of the evolution of both real DI and imaginary DI are similar. In fact, the real DI is linear proportional to imaginary DI. In the previous experimental section, the imaginary DI of 0.05 was set as the threshold for bondline degradation, which was corresponding to an interfacial loss of 20%. The imaginary DI of 0.40, a typical value observed right before the adhesive failure of the bondline, was corresponding to an interfacial loss of 80%.

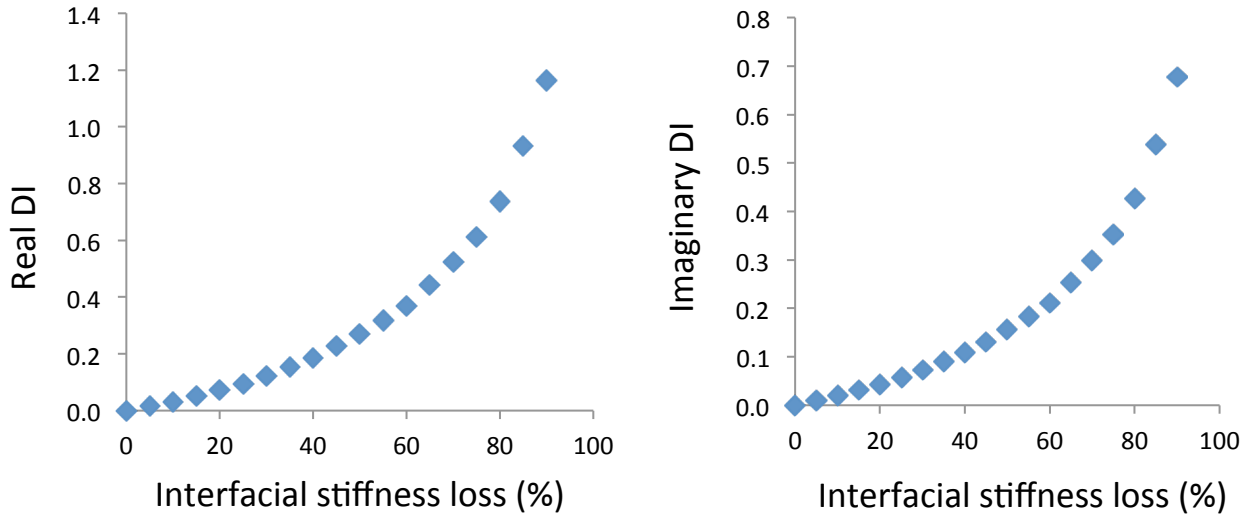


Figure 8: With the increase of the stiffness loss of the interfacial element, the damage index of (left) real impedance and (right) imaginary impedance will increase dramatically

### 3.3 Design of miniaturized sensors

In order to embed the piezoelectric sensor into the bondlines, the sensor should be miniaturized in order to minimize the parasitic effect on the bondline’s mechanical performance. With the finite element simulation, the parametric study was conducted to investigate the effect of sensor’s diameter and thickness on the impedance behavior of the embedded piezoelectric sensor. The dependency of impedance on the thickness was plotted in Figure 9. Three levels of thickness were investigated and the diameter was fixed at 3 mm. With the decrease of the thickness of the embedded piezoelectric sensor, the peak impedance will go down while the resonant frequency is constant. In practice, the impedance analyzer with higher resolution would be desired in order to compensate the decreased value of impedance. The dependency of impedance on the diameter was also plotted in Figure 10. Three levels of diameter were also investigated while the thickness was fixed at 3 mm. With the decrease of the diameter of the embedded piezoelectric sensor, the peak impedance will increase and the resonant frequency will increase as well. The increase of impedance and the frequency is preferable for the bondline integrity monitoring for the higher sensitivity of impedance analyzer and the capability to find smaller degradation in bondlines.

## 4. CONCLUSIONS

Compared to conventional bolted joints, bonded joints have superior mechanical properties in terms of light weight, less stress concentration, etc. However, due to the lack of confidence on the bondline integrity level during fabrication and service, the large adaption of bonded joints onto airplane primary structural components is restricted by regulations and standards. Among all the defects that can be found in adhesive bondlines, one type of interfacial weakness, the kissing bond, is the most challenging one. This is due to the catastrophic failure it can cause to the bondline as well as to the almost impossible early detection using conventional non-destructive evaluation (NDE) or structural health monitoring (SHM) techniques.

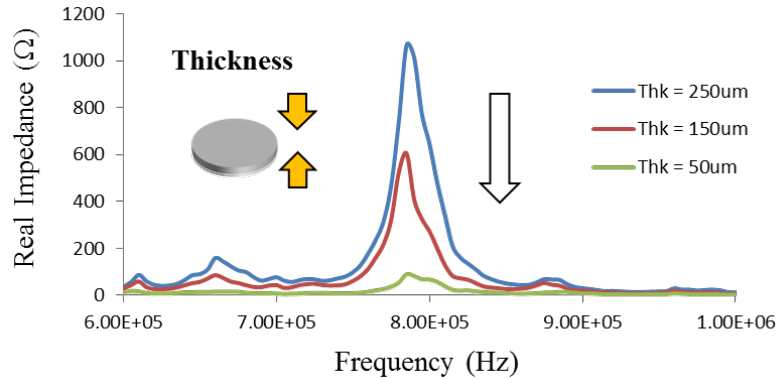


Figure 9: The resonant peak of the real impedance will decrease and the frequency will keep constant when decrease the thickness of the embedded piezoelectric disc sensor

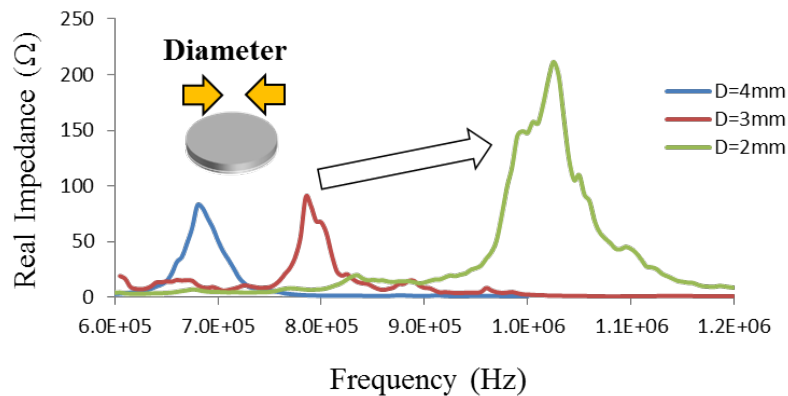


Figure 10: The resonant peak of the real impedance will increase and the frequency increase as well when decrease the diameter of the embedded piezoelectric disc sensor

We developed and tested a break-through technique to monitor the bondline integrity by embedding piezoelectric sensors into the bonded joints. The impedance-based detection algorithms were used by measuring the electromechanical impedance of the embedded sensors. Since the sensors are positioned in the bondlines, close to the interface of adhesive and adherent, where the kissing bond could occur, any small change in the interface would affect the EMI response of the sensor. The EMI behavior of the embedded sensor under static loading was studied before and the behavior under fatigue loading was presented in this work. The impedance was recorded under zero load condition after a fixed number of load cycles. A similar behavior as the static loading was observed, i.e. the impedance of the sensor is kept constant until a certain fatigue cycles, after which, the impedance changes dramatically from the pristine state. The root mean square deviation was defined as the damage index to quantify the change of impedance.

A finite element model was also developed to investigate the impedance behavior of the embedded piezo sensor. In order to simulate the behavior of kissing bond, the stiffness of the interface elements of the adhesive was degraded. The degradation of this 10  $\mu\text{m}$  thick element would not affect the global stiffness of the lap joint. However, it would affect the impedance behavior of the embedded sensors significantly. Preliminary simulation results matched with the experimental result qualitatively and similar trend of the decrease of resonant frequency was seen when the sample was prone to failure.

The finite element simulation was also used as an optimization tool to miniaturize the dimensions of the sensor's design and to increase the sensitivity of the sensor as well. A break-through technique of fabricating thin film sensor of

piezoelectric ceramic material was developed. The thickness of the sensor can be as low as 10  $\mu\text{m}$ , which makes it an ideal solution of the sensor to be embedded in the bondlines. Future work will include the improvement on the screen-printing techniques for the impedance-based algorithms for bondline integrity monitoring.

## 5. ACKNOWLEDGEMENT

This research was supported by the Boeing Company under the contract 9010406 and Air Force Office of Scientific Research under the contract FA9550-13-1-0139. This work is also partially support from Multidisciplinary University Research Initiative project under the contract FA9550-09-1-0677.

## REFERENCES

- [1]. Achenbach, J.D., & Parikh, O.K. "Ultrasonic Analysis of Nonlinear Response and Strength of Adhesive Bonds." *J. Adhes. Sci.* 5(8) (1991): 601-608
- [2]. Baltazar, A., Rokhlin, S.I., & Pecorari, C. "The Relationship between Ultrasonic and Micromechanical Properties of Contacting Rough Surfaces" *J. Mech. Phys. Solids* 50(2002): 1397-1416
- [3]. Baltazar, A., Wang, L., Xie, B., & Rokhlin, S.I. "Inverse Ultrasonic Determination of Imperfect Interfaces and Bulk Properties of A Layer between Two Solids." *Acoustical Society of America*. 114 (3)(2003): 1424-1434
- [4]. Brotherhood, C.J., Drinkwater, B.W., & Dixon, S. "The Detectability of Kissing Bonds in Adhesive Joints Using Ultrasonic Techniques." *Ultrasonic* 41(7) (2003): 521-529
- [5]. Eehart, B., Valeskes, B., Muller, C.E., Bockenheimer, C. "Methods for the Quality Assessment of Adhesive Bonded CFRP Structures -A Resumé." *2nd International Symposium on NDT, Aerospace 2010, We.5.B.2*
- [6]. Ihn, J.B., & Chang, F.K. "Built-in Diagnostics for Monitoring Crack Growth in Aircraft Structures" *Proceedings of the 3rd international Workshop on Structural Health Monitoring*. Stanford, CA, Sept 2001 pp. 284-295
- [7]. Ihn, J.B., & Chang, F.K. "Hot Spot Monitoring for Aircraft Structures", *Advanced Smart Materials and Smart Structures Technology*. 2004
- [8]. Ihn, J.B., & Chang, F.K. "Detection and Monitoring of Hidden Fatigue Crack Growth Using a Built-in Piezoelectric Sensor/actuator Network." *Smart Material Structure* 13(2004): 609-620
- [9]. Jiao, D., & Rose, J.L. "An Ultrasonic Interface Layer Model for Bond Evaluation." *J. Adhesion Science and Technology* 5(8) (1991): 631-646
- [10]. Light, G.M., & Kwun, H. "Nondestructive Evaluation of Adhesive Bond Quality, State-of-the-Art Review." *NTIAC* 89(1) (1989)
- [11]. Maeva, E., Severina, I., Bondarenko, S., Chapman, G., O'Neil, B., Severin, F., & Maev, R. Gr. "Acoustical methods for the investigation of adhesively bonded structures: A review." *Can. J. Phys.* 82(2004): 981-1025
- [12]. Margetan, F.J., Thompson, R.B., & Gray, T.A. "Interfacial Spring Model for Ultrasonic Interactions with Imperfect Interfaces: Theory of Oblique Incidence and Application to Diffusion-Bonded Butt Joints." *Journal of Nondestructive Evaluation*. 7 (3-4) (1988)
- [13]. Nagy, P.B. "Ultrasonic Classification of Imperfect Interfaces." *J. Adhesion Science and Technology* 5(1991): 619-630
- [14]. Rokhlin, S.I., Wang, L., Xie, B., Yakovlev, V.A. & Adler, L. "Modulated Angle Beam Ultrasonic Spectroscopy for Evaluation of Imperfect Interfaces and Adhesive Bonds." *Ultrasonic* 42 (2004): 1037-1047.
- [15]. Rokhlin, S.I., Xie, B., & Baltazar, A. "Quantitative Ultrasonic Characterization of Environmental Degradation of Adhesive Bonds." *J. Adhesion Sci. Technol.* 18(3)(2004): 327-359

- [16]. Tang, Z., Cheng, A., & Achenbach, J.D. "An Ultrasonic Technique to Detect Nonlinear Behaviour Related to Degradation of Adhesive Joints." *QNDE*, D.O. Thompson, D.E. Chimenti (Eds), Vol. 17, Plenum Press, New York, 1998.
- [17]. Wang, N., Lobkis, O. I., Rokhlin, S. I., & Cantrell, J. H. "Ultrasonic Characterization of Interfaces in Composite Bonds." *AIP Conf. Proc.* 1335, 1079 (2011)
- [18]. Zhuang, Y., Kopsaftopoulos F.P., Chang F.-K., "Bondline integrity monitoring of adhesively bonded structures via an electromechanical impedance based approach", *Proceedings of the 10th International Workshop on Structural Health Monitoring (IWSHM)*, Stanford University, USA, September 2015.
- [19]. Salowitz, N., Guo, Z., Kim, S.-J., Li, Y.-H., Lanzara, G., Chang, F.-K., "Micro-fabricated expandable sensor networks for intelligent sensing materials", Invited Paper, accepted in *IEEE Sensors*, DOI: 10.1109/JSEN.2013.2297699.
- [20]. Salowitz N., Guo Z., Li Y.-H., Kim K., Lanzara G., and Chang F.-K., "Bio-Inspired Stretchable Network Based Intelligent Composites", Invited paper, *Journal of Composite Materials*, vol. 47(1), pp. 97-105.